Investigation of the Connectivity of Hydrophilic Domains in Nafion Using Electrochemical Pore-Directed Nanolithography

Daniel J. Gargas, David A. Bussian, and Steven K. Buratto*

Department of Chemistry and Biochemistry, University of California, Santa Barbara, California 93106

ABSTRACT

A method of determining the connectivity of ion-conducting hydrophilic channels within the Nafion polymer electrolyte membrane by way of pore-directed nanolithography has been developed. Electrochemical etching of a silicon surface is performed through a Nafion-membrane mask. The resulting silicon surface imaged by tapping-mode atomic force microscopy (TMAFM) provides a footprint of the hydrophilic channels at the Nafion-silicon interface. In a similar fashion, a TMAFM phase-contrast image of the top surface of the Nafion mask prior to etching reveals the spatial distribution of hydrophilic domains at the surface of the polymer membrane. Collectively, these images provide detailed information about the structure of the hydrophilic channels at the top and bottom surfaces of the Nafion membrane. Autocorrelation statistical analysis of these two sets of images shows that only 48% of hydrophilic channels beginning at the Nafion surface connect to the silicon-Nafion interface.

The development of polymer electrolyte fuel-cell technology garnered significant research interest as robust ionomer membranes became available in the 1970s.[1] A variety of proton exchange membranes (PEM) with enhanced stability, proton conductivity, and processibility derive their properties from the ability of the parent copolymers to form biphasic solids with nanoscopic regions of high hydrophilicity and acidity nested within an inert semirigid matrix.[2−4] To date, perfluoronated sulfonic acid polymers have experienced the most widespread use in commercial applications.[5,6] A classic example of this type is the Nafion group of polymers produced by DuPont. Membranes of these polymers have been studied intensively, and much is known about the effects of hydration, temperature, and wear on their performance.[7−9] Little is known, however, about the internal structure of the nanoscopic aqueous domains that mediate proton transport.[10−12] Recent experiments using electrochemical deposition of metal through Nafion membranes and subsequent imaging of the metal-decorated surface has provided new insight into the footprint of the hydrophilic channels at the Nafion/substrate interface.[13] These experiments, however, do not provide any information regarding connectivity of the pore channels. The number, connectivity, and conductivity of these domains are critical to understanding the mechanism of proton transport

Figure 1. Schematic drawing of a Nafion polymer membrane with hydrophilic channels (white) affixed to a silicon substrate (black). A percentage of the channels traverse the entire membrane, allowing electrochemical etching at the Nafion/silicon interface. This method of selective electrochemical etching initiates porous silicon (speckled gray) at the location of the hydrophilic channels.

and can ultimately prove to be useful in creating new membranes with enhanced conductivity.

We have developed a novel methodology for determining the nanoscale connectivity of aqueous surface states through PEMs. Our initial studies are focused on the well-characterized Nafion membrane. To determine the number of aqueous domains that contiguously span the membrane, we utilized silicon etching protocols with the addition of the Nafion membrane as a mask. In this procedure, a Nafion membrane is affixed to a silicon substrate and then the underlying silicon is selectively electrochemically etched (Figure 1). This

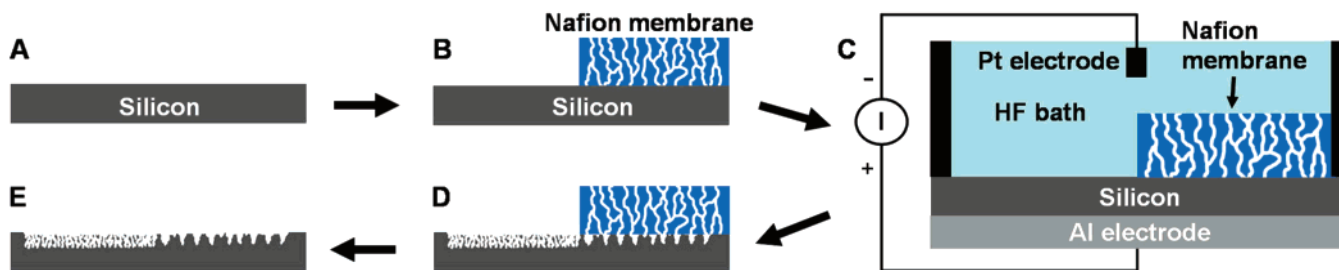* Corresponding author. E-mail: buratto@chem.ucsb.edu.

Figure 2. (A) Silicon wafer is prepared by sonication in piranha solution (3:1 H_2SO_4/30% H_2O_2) and rinsing with 15% HF for oxide removal, (B) Nafion layer is deposited by dip-coating into a suspension of 5% Nafion (equiv wt 1100) in lower aliphatic alcohols, (C) anodic etching occurs inside an electrochemical cell with 15% HF/H_2O solution at a constant current density between 0.1 and 1.0 mA/cm², (D) surface regions of Nafion-masked silicon are etched only at the end of a hydrophilic channel because HF transport occurs only within hydrophilic channels of the Nafion membrane, (E) the Nafion layer is removed with ethanol, and the sample is cleaned and dried under N_2.

approach takes advantage of silicon as a flat substrate, as well as the diffusion of etching species occurring only through the hydrophilic domains of the Nafion membrane. Removal of the Nafion mask allows the morphology of etched silicon to be fully characterized via standard scan probe and electron microscopy. This appears to provide a useful measurement of the density of conductive aqueous domains. In addition, the top surface of Nafion can be imaged with domain-sensitive scan probe techniques to quantify the density and extent of the entrance channels.[14−18]

Silicon wafers (p-type [100] 0.01 Ω cm 500-μm thickness, University Wafer) were cut into 1-cm² samples, sonicated in piranha solution (3:1 H_2SO_4/30% H_2O_2), rinsed with 15% HF to remove surface oxide, rinsed in ethanol, and dried under N_2 air. Nafion films were prepared by dipping silicon samples halfway into Nafion alcohol solution (eq. wt. 1100, Aldrich), creating a Nafion film roughly 2−3 μm thick over half of the sample surface. Teflon-masked samples were fabricated by adhering 0.5-cm² sections of Teflon film (FEP Type 50A, 12.5-μm thickness, DuPont) to silicon samples using a 1-μL aliquot of Nafion alcohol solution as an adhesive. All of the samples were made so that half of the silicon surface was masked and half was exposed (Figure 2). Samples were anodically etched in an electrochemical cell[19] using a 15% HF/H_2O solution with applied currents between 0.1 and 1 mA/cm² for time periods of 15−180 s. Subsequent Nafion removal was realized by sonication in piranha solution and rinsing in ethanol. Surface images were obtained by scanning electron microscopy (JEOL 6300F SEM operating at 5 kV accelerating voltage) and atomic force microscopy (Digital Instruments Nanoscope IIIa SPM). Elemental analysis was obtained using an environmental scanning electron microscope equipped with an energy-dispersive spectrometer (Princeton Gamma Tech).

Anodic etching of silicon with a hydrofluoric species creates a porous network on the silicon surface with pore dimensions well within the resolution limits of scan probe microscopy.[20,21] Tapping-mode AFM (TMAFM) images of bare-etched silicon reveal a significant change in surface morphology after anodic etching (Figure 3A). The resulting surface topography is attributed to the creation of siloxene within the porous silicon framework.[22,23] The lower density of siloxene causes expansion of the lattice, resulting in slight undulations at the surface that are referred to as hillocks
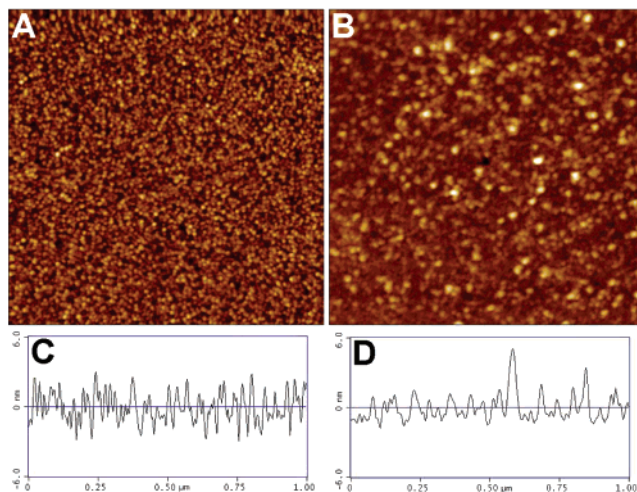

Figure 3. TMAFM height images (1 × 1 μm² scan size) of (A) etched silicon and (B) etched Nafion-masked silicon (height scale is 12 nm). Cross-section plots are shown in C and D. Samples were anodically etched in 15% HF/H_2O for 3 min at 0.6 mA/cm² current density.

elsewhere.[21,24−27] This effect is observed in cross-section plots showing surface features 3−5 nm high and roughly 10−20 nm wide (Figure 3C).

Silicon etched through Nafion, however, exhibits a remarkable difference in surface roughness and feature height compared to bare-etched silicon. TMAFM images reveal a much lower density of surface features on the etched silicon surface (Figure 3B). The contrast in surface feature size and distribution is seen clearly in cross-section plots (Figure 3D). The unmasked silicon regions show a uniform distribution of features roughly 10−20 nm wide and 3−5 nm high, signifying an isotropic etching environment, whereas Nafion-masked regions exhibit a random distribution of features approximately 20−30 nm in width and 2−3 nm in height. The contrast in surface morphology was also observed by scanning electron microscopy (Figure 4). Complete Nafion removal from etched samples was confirmed by elemental analysis via energy dispersion spectroscopy, which eliminates Nafion residue as the cause of surface features observed by scan probe microscopy. In addition, no surface morphology was observed on equivalently etched Teflon-masked silicon samples, which eliminates the possibility of ion transport through hydrophobic domains of the Nafion membrane.
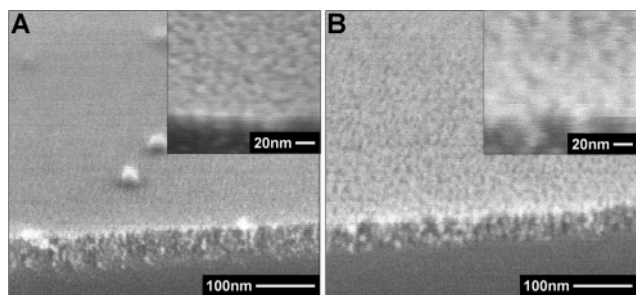
Figure 4. SEM cross-section images of etched silicon: (A) unmasked region (B) Nafion-masked region. Insets show magnified regions of the surface.

The discrepancy in surface topography between etched silicon and Nafion-masked silicon samples is attributed to localized etching through the hydrophilic domains of the Nafion mask. The top side of the Nafion mask is in contact with the HF etching solution, and the other side is in contact with the silicon surface forming a Nafion/silicon interface. A hydrophilic domain must be in contact with the silicon surface in the interfacial region in order for etching to occur. This same domain must also be connected to the top of the Nafion mask through a hydrophilic channel. HF transport occurs only within hydrophilic channels of the Nafion membrane and, therefore, is dependent on the connectivity of such channels.[28] Surface regions of Nafion-masked silicon are exposed to HF and subsequently etched only at the end of a hydrophilic channel. These areas exhibit a significant change in surface topography after etching. In contrast, interface regions in contact with the hydrophobic domains experience minimal HF exposure and, therefore, exhibit little or no surface morphology. As a result, a direct correlation between the footprint of an etched silicon surface and the channel connectivity within the Nafion membrane is understood.

As discussed above, a TMAFM height image of the silicon surface after Nafion-masked electrochemical etching provides a model of the hydrophilic channel structure at the silicon−Nafion interface. In a similar fashion, a TMAFM phase-contrast image of the top surface of Nafion reveals the spatial distribution of hydrophilic domains at the surface of the polymer membrane.[14−16] Collectively, these images provide detailed information about the structure of hydrophilic channels at the top and bottom surfaces of the Nafion membrane (Figure 5). Further analysis of the spatial distribution of hydrophilic channels can be obtained from second-order statistical analysis such as the autocorrelation function, $C(r)$

$$C(r) = \frac{1}{w^2} \int [f(x) - \bar{f}(x)][f(x + r) - \bar{f}(x)] \, \mathrm{d}x \quad (1)$$

where w is the RMS value of the TMAFM scan, $f(x)$ and $\bar{f}(x)$ are the value (either height or phase) and average value, respectively, of each scan in the x direction. Because the x axis served as the fast scan axis, values were averaged over the entire scan in the y direction to avoid drift noise. The autocorrelation function plotted versus distance, r, yields a
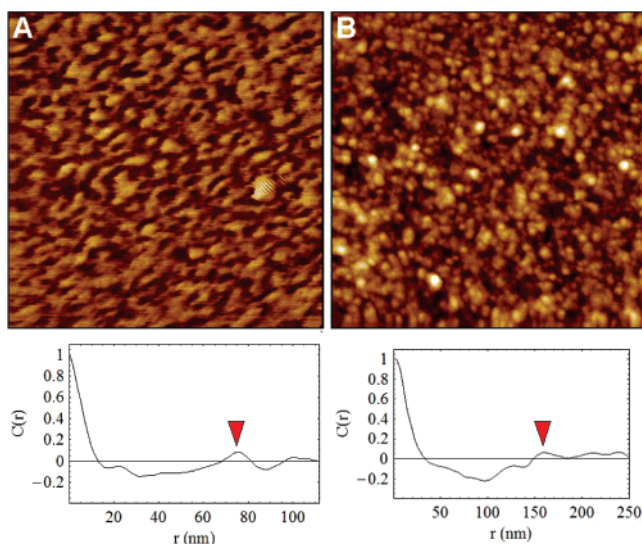

Figure 5. TMAFM images and autocorrelation plots, $C(r)$, are shown for (A) Nafion top surface (phase, 500×500 nm^2) and (B) etched Nafion-masked silicon (height, 1000×1000 nm^2) (phase scale for A is 90°; height scale for B is 12 nm). The plots below show respective correlation lengths (denoted by arrow).

correlation length pertaining to the average spacing between particles of the same value.[29] Thus, autocorrelation function plots of TMAFM scans of the Nafion surface and Nafion-masked silicon surface generate correlation lengths pertaining to the average spacing between hydrophilic channels. Correlation lengths of 75 and 156 nm were determined for the Nafion surface and Nafion-masked silicon surface, respectively (Figure 5). Furthermore, the ratio of hydrophilic channels at the Nafion surface to ion conducting channels observed at the Nafion−silicon interface provides a direct measurement of channel connectivity, or percentage of hydrophilic channels completely traversing the Nafion membrane. The correlation lengths imply that 48% of hydrophilic channels beginning on the Nafion surface connect to the silicon−Nafion interface.

The process of selective electrochemical etching has been demonstrated to be a useful tool in imaging the hydrophilic channels comprising a Nafion polymer membrane. However, this method does not provide insight to the 3D pore structure within Nafion. Our experiments were limited to the nature of entrance and exit channels of hydrophilic domains and could not probe the inner arrangement of ion-conducting channels. Additional experiments must be performed to determine channel properties such as length, shape, and diffusion efficiency.

Our experiments show that it is possible to electrochemically etch silicon through a Nafion membrane and obtain a footprint of the pore structure at the silicon−Nafion interface. Pore sizes observed for Nafion-masked regions were approximately 20−30 nm in width as determined by scan probe microscopy, which agrees well with prior studies of hydrated Nafion.[7,30] It is important to note that the Nafion membranes in our experiments are highly hydrated, and this is reflected in the large size of the hydrophilic domains. Pore sizes in the Nafion membranes are strongly dependent on the method

of preparation and the degree of hydration. Our preparation conditions are different than those in commercial fuel cells, which results in pore channels much larger than those typically observed in working fuel cells. Nonetheless, the connectivity of hydrophilic channels comprising the Nafion membrane was determined by correlating the pore structure of the Nafion film measured by tapping-mode AFM with the footprint at the silicon−Nafion interface. Using auto-correlation statistical analysis, we observed a 48% connectivity of the pores.

References

(1) Mauritz, K. A.; Moore, R. B. *Chem. Rev.* **2004**, *104*, 4535−4585.
(2) Paddison, S. J. *Annu. Rev. Mater. Res.* **2003**, *33*, 289−319.
(3) Kreuer, K. D.; Paddison, S. J.; Spohr, E.; Schuster, M. *Chem. Rev.* **2004**, *104*, 4637−4678.
(4) Ioselevich, A. S.; Kornyshev, A. A.; Steinke, J. H. G. *J. Phys. Chem. B* **2004**, *108*, 11953−11963.
(5) Surampudi, S.; Narayanan, S. R.; Vamos, E.; Frank, H.; Halpert, G.; Laconti, A.; Kosek, J.; Prakash, G. K. S.; Olah, G. A. *J. Power Sources* **1994**, *47*, 377−385.
(6) Chu, Y. H.; Shul, Y. G.; Choi, W. C.; Woo, S. I.; Han, H. S. *J. Power Sources* **2003**, *118*, 334−341.
(7) Chomakovahaefke, M.; Nyffengger, R.; Schmidt, E. *Appl. Phys. A* **1994**, *59*, 151−153.
(8) Heitner Wirguin, C. *J. Membr. Sci.* **1996**, *120*, 1−33.
(9) Hsu, W. Y.; Gierke, T. D. *J. Membr. Sci.* **1983**, *13*, 307−326.
(10) Gierke, T. D.; Munn, G. E.; Wilson, F. C. *J. Polym. Sci., Polym. Phys. Ed.* **1981**, *19*, 1687−1704.
(11) Rollet, A. L.; Diat, O.; Gebel, G. *J. Phys. Chem. B* **2002**, *106*, 3033−3036.
(12) Rubatat, L.; Gebel, G.; Diat, O. *Macromolecules* **2004**, *37*, 7772−7783.
(13) Chou, J.; McFarland, E. W.; Metiu, H. *J. Phys. Chem. B* **2005**, *109*, 3252−3256.
(14) James, P. J.; Antognozzi, M.; Tamayo, J.; McMaster, T. J.; Newton, J. M.; Miles, M. J. *Langmuir* **2001**, *17*, 349−360.
(15) McLean, R. S.; Sauer, B. B. *Macromolecules* **1997**, *30*, 8314−8317.
(16) McLean, R. S.; Doyle, M.; Sauer, B. B. *Macromolecules* **2000**, *33*, 6541−6550.
(17) Lehmani, A.; Durand-Vidal, S.; Turq, P. *J. Appl. Polym. Sci.* **1998**, *68*, 503−508.
(18) Kanamura, K.; Morikawa, H.; Umegaki, T. *J. Electrochem. Soc.* **2003**, *150*, A193-A198.
(19) Mason, M. D.; Sirbuly, D. J.; Buratto, S. K. *Thin Solid Films* **2000**, *406*, 151−158.
(20) Chang, D. C.; Baranauskas, V.; Doi, I.; Prohaska, T. *J. Porous Mater.* **2000**, *7*, 349−352.
(21) Young, T. F.; Huang, I. W.; Yang, Y. L.; Kuo, W. C.; Jiang, I. M.; Chang, T. C.; Chang, C. Y. *Appl. Surf. Sci.* **1996**, *102*, 404−407.
(22) Tischler, M. A.; Collins, R. T. *Solid State Commun.* **1992**, *84*, 819−822.
(23) Tvardauskas, H.; Bukauskaite, B.; Jasutis, V.; Lescinskas, D.; Simkiene, I. *Semicond. Sci. Technol.* **1994**, *9*, 1633−1636.
(24) Kleps, I.; Nicolaescu, D.; Garcia, N.; Serena, P.; Gil, A.; Zlatkin, A. *Ultramicroscopy* **1998**, *73*, 237−245.
(25) Yu, T.; Laiho, R.; Heikkila, L. *J. Vac. Sci. Technol., B* **1994**, *12*, 2437−2439.
(26) Lee, J.; Chakrabarty, K.; Yi, J. *Appl. Surf. Sci.* **2003**, *211*, 373−378.
(27) Dahn, J. R.; Way, B. M.; Fuller, E.; Tse, J. S. *Phys. Rev. B* **1993**, *48*, 17872−17877.
(28) Unnikrishnan, E. K.; Kumar, S. D.; Maiti, B. *J. Membr. Sci.* **1997**, *137*, 133−137.
(29) Zhao, Y.; Wang, G.-C.; Lu, T.-M. *Characterization of Amorphous and Crystalline Rough Surface: Principles* and Applications; Academic Press: San Diego, CA, 2001; Vol. 37.
(30) James, P. J.; McMaster, T. J.; Newton, J. M.; Miles, M. J. *Polymer* **2000**, *41*, 4223−4231.

NL051218S